PROCEEDINGS of the
23rd International Congress on Acoustics
9 to 13 September 2019 in Aachen, Germany

Insulation materials made of renewable raw materials for the sound insulation prognosis of building components

Simon MECKING[(1)]; Andreas RABOLD[(1)]; Anton HUBER[(1)]

[(1)]Technical University of Applied Sciences Rosenheim, Germany, simon.mecking@th-rosenheim.de

Abstract

In order to increase the application possibilities in the building sector for insulating materials made from renewable raw materials, a project was initiated by the *Fachagentur Nachwachsende Rohstoffe e.V.* which shows the different requirements for these insulating materials and provides planning and verification options. In the field of sound insulation, building component catalogues for these insulating materials are expanded, test methods for the material properties of the insulating materials are defined and prediction models are further developed. The airborne and impact sound transmissions of the components are predicted in order to investigate the influence of the different insulating materials from renewable raw materials in comparison to conventional insulating materials. Component measurements indicate that a characterization of the cavity-insulation alone by the flow resistance is insufficient. Using a semi-analytical calculation approach with an equivalent fluid, further insulation material properties can be taken into account in the prognosis of two-shell structural elements. The input data for the prognosis calculation are determined by measurements of the transmission properties and compared with results of other calculation models based on the flow resistance. By validating the first prediction results with measurements, it should be shown to what extent the conventional measured variables are sufficient.

Keywords: Double shell, Transmission, Prediction models, Renewable, Insulation

1 INTRODUCTION

A significant part of the insulation materials used in the construction industry comes from non-renewable raw materials. With regard to adequate recycling and the use of energy during production, insulating materials made from renewable raw materials have some environmental advantages. Within the research project, it will be investigated to what extent the acoustic properties of these insulating materials influence the transmission of airborne sound when used in building components compared to conventional insulating materials.

2 COMPONENT MEASUREMENTS

In a recent project [1] the airborne sound insulation of double walls with various cavity insulations made of renewable raw materials was measured. In addition, the flow resistance (r) and the bulk density (ρ) of the insulating materials were determined. Figure 1 shows the measurement results. The wood fibre and hemp fibre are panel-shaped insulating materials. The cellulose was blown-in and the sea weed was placed manually as loose insulating material.

The measurement results using wood fibre and cellulose show the same weighted sound reduction index despite very different flow resistance. In contrast, hemp fibre and seaweed have the same flow resistance, but sea weed has an airborne sound insulation that is 6 dB smaller. The low frequency transmission loss of the double stud wall with the sea weed is very similar to the variant without insulation material in the cavity. It is assumed that the stiffness of the fibre-skeleton at low frequencies was responsible for the drop in sound insulation.

The results in Fig. 1 show no correlation between the length-related flow resistance and the weighted sound reduction index. This indicates that the acoustic quality of a fibre insulation material is inadequate described purely on the basis of this parameter.

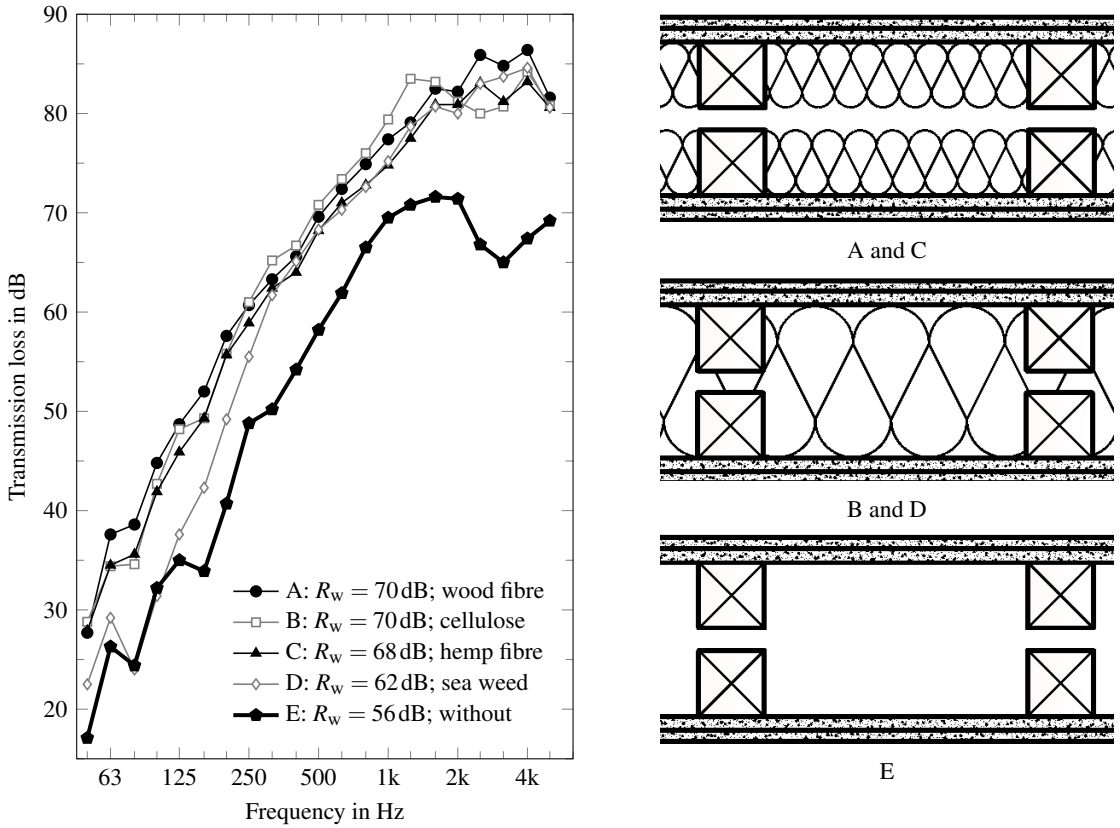

Figure 1. Transmission loss of double stud walls with variation of cavity insulation with measured characteristics (A: $r = 9\,\mathrm{kPa\,s/m^2}$, $\rho = 46\,\mathrm{kg/m^3}$; B: $r = 36\,\mathrm{kPa\,s/m^2}$, $\rho = 58\,\mathrm{kg/m^3}$; C: $r = 3\,\mathrm{kPa\,s/m^2}$, $\rho = 63\,\mathrm{kg/m^3}$; D: $r = 3\,\mathrm{kPa\,s/m^2}$, $\rho = 75\,\mathrm{kg/m^3}$). The double wall consists of wooden studs with two layers 12.5 mm and 10 mm of gypsum fibre boards on each side. The cavity depth is $d \approx 140\,\mathrm{mm}$. The measurements were realized at ift Rosenheim [2].

3 PROGNOSIS FOR DOUBLE-SHELL STRUCTURES WITHOUT CONNECTION

A characteristic parameter in the calculation of sound insulation of double wall constructions is the mass-spring-mass resonance (f_0), which can be calculated according to (1). Thereby m' is the mass per unit area of the two shells and s' is the dynamic stiffness of the cavity filled with insulating material in $\mathrm{N/m^3}$.

$$f_0 = \frac{1}{2\pi}\sqrt{s'\left(\frac{1}{m'_1}+\frac{1}{m'_2}\right)} \tag{1}$$

In a fully description of a porous absorber, the dynamic stiffness is represented by the parts of the skeleton and the fluid in (2) [3].

$$s' = s'_\mathrm{s} + s'_\mathrm{a} \tag{2}$$

The stiffness of air in the pores depends on the dynamic compression modulus ($\underline{K}$) and shell distance (d).

$$s'_\mathrm{a} = \frac{\mathrm{Re}\{\underline{K}\}}{d} \qquad \text{with } p_\mathrm{s} \le \mathrm{Re}\{\underline{K}\} \le \gamma p_\mathrm{s} \tag{3}$$

For isothermal compression, $\mathrm{Re}\{\underline{K}\}$ is equal to the static pressure p_s. This can be assumed for fibrous insulating materials at low frequencies. At high frequencies the compression is adiabatic, increasing $\mathrm{Re}\{\underline{K}\}$ by the adiabatic coefficient (air: $\gamma \approx 1.402$).

3.1 Semi-analytic model

The calculation of the sound insulation for a double wall with sufficient damped cavity can be approximated with (4) and (5) from the transmisson loss of the individual shell [cf. 4, 5]. Both measured values and predicted values of the transmisson loss for the individual panels can be used as input data. The first term in (4) corresponds to Berger's mass law for vertical incidence of sound waves. The sound insulation depends substantially on the mass per unit area of the shells m'_i and the impedance of the air Z_a. The 5 dB in the second term take into account a correction for a practical, diffuse sound field.

$$R = 20\,\lg\left(\frac{\omega\,(m'_1 + m'_2)}{2\,Z_a}\right) - 5\,\mathrm{dB} \qquad (f < f_0) \tag{4}$$

Above the mass-spring-mass resonance, the transmission loss can be calculated approximately according to (5) in case the cavity is filled with a porous absorption material [4, 5].

$$\begin{aligned} R &\approx R_1 + R_2 + 20\,\lg\left(\frac{\omega}{s'}\,\frac{2\,Z_a}{1}\right) \qquad (f > f_0) \\ &\approx R_1 + R_2 + \Delta R \end{aligned} \tag{5}$$

The dynamic stiffness of the interlayer is s' and can be calculated with the frequency-dependent distinction of cases according to (6) [5], if the insulating material has flow resistance of $r \geq 5\,\mathrm{kPa\,s/m^2}$.

$$s' \approx \begin{cases} \dfrac{\rho_a\,{c_a}^2}{d} & (f \leq f_d) \\ \omega\,Z_a & (f > f_d) \end{cases} \tag{6}$$

The change between the calculation methods of the dynamic stiffness of the cavity depends on the wavelength ratio to the shell distance. In [cf. 4–6] the frequency f_d is calculated according (7).[1] After that the transmission loss above f_d increases by 6 dB compared to the sum of the transmission loss of the two individual shells.

$$f_d = \frac{1}{2\pi}\,\frac{c_a}{d} \approx \frac{55}{d} \tag{7}$$

3.2 Modified model

In order to be able to consider the dependency of the characteristic insulation properties in the prediction of airborne sound insulation, a rigid skeleton is assumed in the case of insulating materials that are not loaded by force and an equivalent fluid is assumed as a substitute model. Depending on the shell distance, at medium or higher frequencies cavity resonances (f_{HR}) after (8) can occur, which reduce the sound insulation. Where $\underline{c}$ is the complex phase velocity in the equivalent fluid.

$$f_{HR,n} = n\,\frac{\mathrm{Re}\{\underline{c}\}}{2\,d} \qquad \text{mit} \qquad n = 1, 2, 3\ldots \tag{8}$$

By using a porous absorber the reduction of transmission loss can be minimised. The absorber reduces the stiffness of the air layer and attenuates cavity resonances. In the modified model, the resulting dynamic stiffness is calculated from the superposition A_{res} of the individual cavity resonances multiplied by dynamic stiffness of the equivalent fluid acc. (3). For each resonance, a foot-point excited, damped single-mass oscillator is assumed.

[1] In [5] 4 instead of 2π is given for the transition of the equations, but 2π is also used in the diagram of the source reference. The 2π also results from the crossover frequency of the two equations in (6).

Also the bulk modulus at the mass-spring-mass resonance in (3) and (1) can be determined iteratively with the use of the specific insulation properties of the equivalent fluid. The corresponding values from the standards are additionally shown in Fig. 2. The loss factor (η) for the amplification function A_i of an individual resonance can also be calculated from the dynamic bulk modulus according to (9).

$$\eta = \frac{\mathrm{Im}\{\underline{K}\}}{\mathrm{Re}\{\underline{K}\}} \tag{9}$$

To correct the difference in impedance between air and the cavity filled with insulating material, a further ratio between these impedances is added in (10). With decreasing frequency the influence of this correction on the result increases. The difference caused by the impedance correction is exemplarily shown in Figure 3.

$$\begin{aligned} R &\approx R_1 + R_2 + 20\,\mathrm{lg}\left(\frac{\omega\,\Phi}{s'_\mathrm{a}\,A_\mathrm{res}}\,\frac{2\,Z_\mathrm{a}}{1}\,\frac{Z_\mathrm{a}}{\mathrm{Re}\{\underline{Z_\mathrm{c}}\}}\right) \\ &\approx R_1 + R_2 + \Delta R_\mathrm{modified} \end{aligned} \tag{10}$$

3.3 Equivalent fluids

For this approach, it is assumed that the fibre-skeleton is rigid, is not shifted and the coupling between skeleton and fluid is negligible. If there are doubts, a complete poroelastic model should be used. The dynamic bulk modulus of the absorber is calculated according to (11) from the characteristic wave impedance ($\underline{Z_\mathrm{c}}$) and the propagation coefficient ($\underline{\gamma}$) or the complex phase velocity ($\underline{c}$) [see 7, 8].

$$\underline{K} = \mathrm{j}\,\omega\,\frac{Z_\mathrm{c}}{\underline{\gamma}} = \underline{c}\,\underline{Z_\mathrm{c}} \tag{11}$$

3.3.1 Semi-empiric models for fibre absorbers

The characteristic impedance and the propagation coefficient can be calculated on the basis of the flow resistance using semi-empirical models for fibre materials [cf. 9–11] according (12) and (13). The basis of the different fit parameters in the models are regression analyses of measurement results from glass wool and rock wool samples, which often show a porosity close to one.

$$\underline{Z_\mathrm{c}} = R + \mathrm{j}X$$

$$= Z_\mathrm{a}\left(1 + 0.0497\left(\frac{f}{r}\right)^{-0.754}\right) + \mathrm{j}\left[Z_\mathrm{a}\left(-0.0758\left(\frac{f}{r}\right)^{-0.732}\right)\right] \quad [9] \tag{12a}$$

$$= Z_\mathrm{a}\left(1 + 0.0699\left(\frac{f}{r}\right)^{-0.632}\right) + \mathrm{j}\left[Z_\mathrm{a}\left(-0.107\left(\frac{f}{r}\right)^{-0.632}\right)\right] \quad [10] \tag{12b}$$

$$= Z_\mathrm{a}\left(1 + 0.00027\left(2 - \mathrm{lg}\,\frac{f}{r}\right)^{6.2}\right) + \mathrm{j}\left[Z_\mathrm{a}\left(-0.0047\left(2 - \mathrm{lg}\,\frac{f}{r}\right)^{4.1}\right)\right] \quad [11] \tag{12c}$$

$$\underline{\gamma} = \alpha + \mathrm{j}\beta$$

$$= \frac{\omega}{c_\mathrm{a}}\left[0.169\left(\frac{f}{r}\right)^{-0.595}\right] + \mathrm{j}\frac{\omega}{c_\mathrm{a}}\left[1 + 0.0858\left(\frac{f}{r}\right)^{-0.700}\right] \quad [9] \tag{13a}$$

$$= \frac{\omega}{c_\mathrm{a}}\left[0.160\left(\frac{f}{r}\right)^{-0.618}\right] + \mathrm{j}\frac{\omega}{c_\mathrm{a}}\left[1 + 0.109\left(\frac{f}{r}\right)^{-0.618}\right] \quad [10] \tag{13b}$$

$$= 0.0069\,\frac{\omega}{c_\mathrm{a}}\left(2 - \mathrm{lg}\,\frac{f}{r}\right)^{4.1} + \mathrm{j}\frac{\omega}{c_\mathrm{a}}\left[1 + 0.0004\left(2 - \mathrm{lg}\,\frac{f}{r}\right)^{6.2}\right] \quad [11] \tag{13c}$$

3.3.2 Macroscopic model for fibre absorbers

A more sophisticated prognosis under consideration of further macroscopic parameters is the calculation of the characteristic impedance and the propagation coefficient according to Johnsen-Champoux-Allard (JCA) [8, 12] in (14) and (15). In addition to the flow resistance, the porosity Φ, the tortuosity τ, the viscous and the thermal length (Λ, Λ') of the insulating materials are also taken into account. In describing the air, the Prandtl number Pr and the dynamic viscosity μ are also required.

$$\underline{K}(\omega) = \gamma p_\mathrm{s} \left[\gamma - \frac{(\gamma - 1)}{\left(1 + \frac{\Phi r'}{\mathrm{j}\tau Pr \rho_\mathrm{a} \omega} \sqrt{1 + \frac{\mathrm{j}4\mu\tau^2 Pr \rho_\mathrm{a} \omega}{\Phi^2 \Lambda'^2 r'^2}} \right)} \right]^{-1} \tag{14}$$

$$\underline{\rho}(\omega) = \rho_\mathrm{a} \tau \left[1 + \frac{\Phi r}{\mathrm{j}\tau \rho_\mathrm{a} \omega} \sqrt{1 + \frac{\mathrm{j}4\mu\tau^2 \rho_\mathrm{a} \omega}{\Phi^2 \Lambda^2 r^2}} \right] \tag{15}$$

In Fig. 2 dynamic bulk modules, loss factors and phase velocities resulting from the macroscopic and semi-empirical models are presented for the parameter data sets 1 and 2 of Tab. 1.

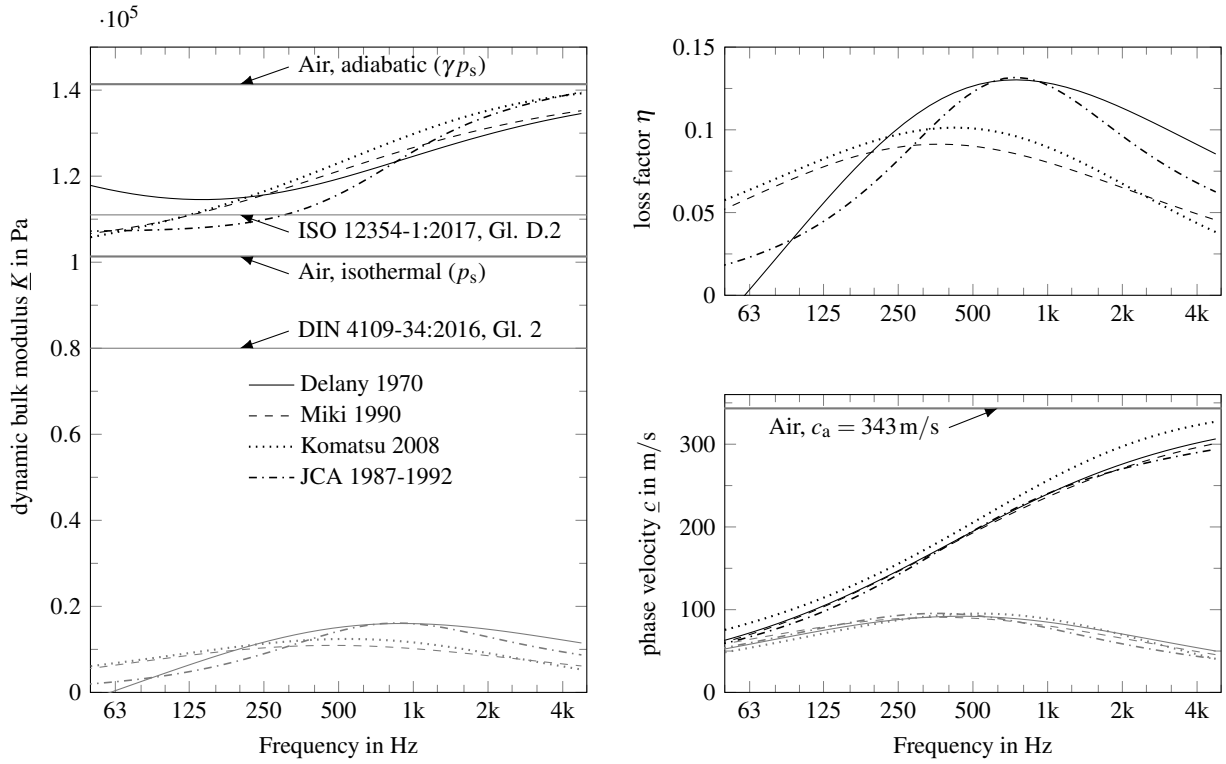

Figure 2. Properties of equivalent fluids calculated acc. to empirical models [9–11] for Par. 2 and a macroscopic model acc. to Johnson-Champoux-Allard (JCA) [12, 13] for Par. 1 from Tab. 1. The imaginary parts are grey.

3.4 Application

Figure 3 shows the influence of the cavity from the modified calculation compared to that of the semi-empirical approach [4, 5] and to the values [15] obtained from measurements. The modified prediction shows a better agreement to the measurement results in the frequency range of cavity resonances. The significant reductions in

Table 1. Characteristics of insulation materials.

	r	Φ	τ	Λ	Λ'
	$\mathrm{kPa\,s/m^2}$			µm	µm
Par. 1 [14]	5.20	0.95	1.00	131	187
Par. 2	5.20				
Par. 3 [14]	11	0.94	1.40	58	122

sound insulation are probably due to the fact that only the vertical sound incidence was taken into account in the prediction. The double-shell wall consisted of two 16 mm chipboards and a mineral fibre insulation in the cavity. To calculate the equivalent fluid, the empirical model according to [11] was used with a flow resistance of $r = 5.2\,\mathrm{kPa\,s/m^2}$ (Par. 2) .

Figure 4 shows the resulting transmission loss from the measurements against two different parameter data sets for the insulation material using the modified calculation. The type of insulation material can lead to significant differences in transmission loss.

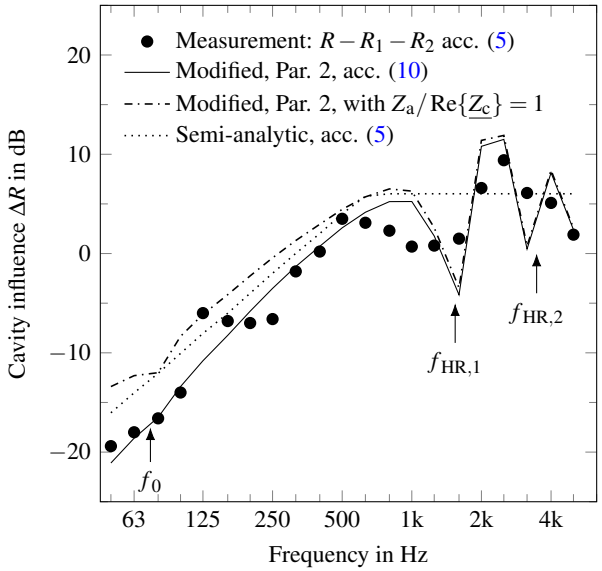

Figure 3. Cavity influence ΔR according to modified model with properties of equivalent fluid (Par. 2 from Tab. 1) according to [11] compared to the semi-analytical approach [4, 5] and the values determined from measurements [15].

4 CONCLUSIONS

With the modified prediction model, the transmission loss through the cavity resonances and the mass-spring-mass resonance can be calculated using amplification functions of a damped oscillator with a single degree of freedom. The equivalent fluids used for this purpose make it possible to calculate these depending on the characteristics of the insulating material. This makes it possible to evaluate the acoustic quality of insulating materials made from renewable raw materials in comparison to conventional insulating materials.

The next steps are to use insulation properties determined by measurement at PTB Braunschweig [cf. 16] as input data for the prognosis and to compare them with component measurements. In addition, the transmission via studs will be integrated into the prognosis.

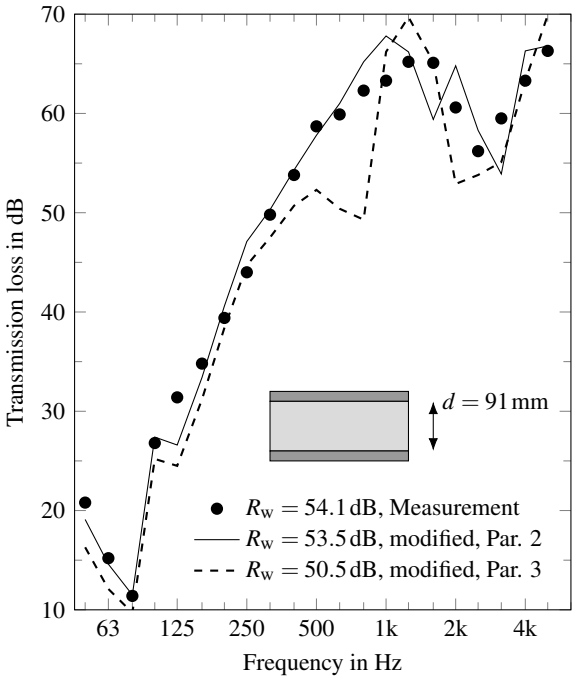

Figure 4. Predicted transmission loss for two insulation material parameter datasets (Par. 2 and 3 from Tab. 1) compared to measurements [15].

ACKNOWLEDGEMENTS

The results are from subproject 3 of the joint research project *Mehr als nur Dämmung - Zusatznutzen von Dämmstoffen aus nachwachsenden Rohstoffen* funded by Bundesministerium für Ernährung und Landwirtschaft (BMEL) via Fachagentur Nachwachsende Rohstoffe e.V. (FNR) with the funding code 22005516.

REFERENCES

[1] Forschungsverbundprojekt: Mehr als nur Dämmung - Zusatznutzen von Dämmstoffen aus nachwachsenden Rohstoffen - Teilbereich Schallschutz von TH Rosenheim; PTB Braunschweig: in Bearbeitung

[2] Huber, A.: Ermittlung von Planungsdaten für den Schallschutz von Außenwänden in Holzbauweise mit unterschiedlichen Dämmstofftypen: Datensammlung - Bauteilmessung - Simulation. Bachelorarbeit. Hochschule Rosenheim, 2018

[3] Cremer, L.; Heckl, M. A.: Körperschall: Physikalische Grundlagen und Anwendungen. Berlin, Heidelberg, New York: Springer Verlag, 1967

[4] Sharp, B. H.: Prediction methods for the sound transmission of building elements. Noise Control Engineering Journal 11.2 (1978), pp. 53–63

[5] Gösele, K.: Zur Berechnung der Luftschalldämmung von doppelständigen Bauteilen (ohne Verbindung der Schalen). Acta Acustica 45.4 (1980), pp. 218–227

[6] Vér, I. L.: "Interaction of sound waves with solid structures: Chapter 11". In: *Noise and vibration control engineering*. Ed. by Vér, I. L.; Beranek, L. L. Hoboken, N.J: Wiley, 2006

[7] Beranek, L. L.: Acoustical Properties of Homogeneous, Isotropic Rigid Tiles and Flexible Blankets. J. Acoust. Soc. Jap. (E) 19.4 (1947), pp. 556–568

[8] Allard, J. F.; Champoux, Y.: New empirical equations for sound propagation in rigid frame fibrous materials. J. Acoust. Soc. Am. 91.6 (1992), pp. 3346–3353

[9] Delany, M. E.; Bazley, E. N.: Acoustical properties of fibrous absorbent materials. Appl. Acoust. 3.2 (1970), pp. 105–116

[10] Miki, Y.: Acoustical properties of porous materials - Modifications of Delany-Bazley models. J. Acoust. Soc. Jpn. (E) 11.1 (1990), pp. 19–24

[11] Komatsu, T.: Improvement of the Delany-Bazley and Miki models for fibrous sound-absorbing materials. Acoust. Sci. Technol. 29.2 (2008), pp. 121–129

[12] Johnson, D. L. et al.: Theory of dynamic permeability and tortuosity in fluid-saturated porous media. J. Fluid. Mech. 176.-1 (1987), p. 379

[13] Champoux, Y.; Allard, J.: Dynamic tortuosity and bulk modulus in air–saturated porous media. J. Appl. Phys. 70.4 (1991), pp. 1975–1979

[14] Glé, P. et al.: Acoustic performance prediction for building elements including biobased fibrous materials. In: *Proc. of Euronoise 2018*. (May 27–31, 2018). Crete, Greece, 2018

[15] Nusser, B.: Entwicklung bauakustisch optimierter Trennwände aus Leichtbauplatten auf Basis gewonnener Materialkennwerte. Masterarbeit. Hochschule Rosenheim, 2007

[16] Wittstock, V.; Sgrieß, D.: Experimental characterisation of absorbing materials made from renewables. In: *Proc. of ICA*. (Sept. 9–13, 2019). Aachen, Germany, 2019